Arene–perfluoroarene interactions in crystal engineering 8: structures of 1:1 complexes of hexafluorobenzene with fused-ring polyaromatic hydrocarbons†‡

Jonathan C. Collings,[a] Karl P. Roscoe,[a] Edward G. Robins,[a] Andrei S. Batsanov,*[a] Lorna M. Stimson,[a] Judith A. K. Howard,[a] Stewart J. Clark[b] and Todd B. Marder*[a]

[a] *Department of Chemistry, University of Durham, South Road, Durham, UK DH1 3LE. E-mail: Todd.Marder@durham.ac.uk, A.S.Batsanov@durham.ac.uk; Fax: +44(191)-384-4737; Tel: +44(191)-374-3137*

[b] *Department of Physics, University of Durham, South Road, Durham, UK DH1 3LE*

Received (in London, UK) 17th July 2002, Accepted 10th October 2002
First published as an Advance Article on the web 5th November 2002

A series of 1:1 complexes of hexafluorobenzene (HFB) with naphthalene, anthracene, phenanthrene, pyrene and triphenylene were prepared and their X-ray crystal structures determined at low temperatures. Each structure contains infinite mixed stacks of alternating nearly-parallel molecules of HFB and arene, which display various 'slip' distortions and form different 3-dimensional motifs. The naphthalene, anthracene and pyrene complexes show polymorphism. Crystal packing of HFB complexes is compared with that of corresponding octafluoronaphthalene complexes. *Ab initio* DFT calculations on the infinite lattices give lattice parameters and 'slip' parameters in close agreement with the experimental crystal structures, while showing that intermolecular cohesion is predominantly of electrostatic, rather than van der Waals, origin.

Introduction

Perfluoroarenes, particularly hexafluorobenzene (HFB), are well-known to co-crystallise with arenes and their derivatives in the form of 1:1 molecular complexes, with nearly-parallel molecules stacked alternately in the solid state (for an up-to-date survey of the literature, see ref. 2). These complexes are of substantial theoretical interest as to the nature of forces governing their structure,[3,4] and of actual or potential importance for solid-state polymerisation[5a,b] and cross-linking of hydrogels,[5c] molecular electronics and photonics[6] and liquid-crystal stabilisation.[7] The HFB solvate of hexamelamine shows anticancer activity.[8]

The first complex of this type was obtained serendipitously by Patrick and Prosser[9] from liquid HFB (mp 5.0 °C) and benzene (mp 5.4 °C) as a solid of mp 23.7 °C. Difficulties of crystallising HFB·benzene and its complicated polymorphism[10] delayed the unequivocal elucidation of its crystal structure[11] until 1992. Meanwhile, complexes of HFB with methyl-substituted arenes (*p*-xylene, mesitylene, durene and hexamethylbenzene)[12] were studied crystallographically and shown to be comprised of mixed stacks of nearly, but not strictly, parallel alternating molecules of HFB and arene, in stark contrast with the herringbone (edge-to-face) crystal packing of pure HFB,[13] as well as the majority of pure arenes.[14] The same one-dimensional motif (the mixed stack) occurs in every other studied arene-perfluoroarene complex, although these stacks can combine into quite different 3-dimensional patterns. Thus, we found[2] that complexes of octafluoronaphthalene (OFN) with anthracene, phenanthrene, pyrene and triphenylene have very similar crystal packings, which differ substantially from that of OFN·naphthalene.[15] On the other hand, the latter complex, OFN·1,8-diaminonaphthalene,[16] OFN·acenaphthene[1] and OFN·1-fluoronaphthalene[17] give isostructural (pseudo-isomorphous) crystals. Thus, there are discreet stable patterns, which persist even as the disparity of size and form between the arene and perfluoroarene molecules increases.

The nature of intermolecular forces responsible for this remains a subject of controversy. Both refractometry[18] and spectroscopy[8] show the absence of any intermolecular charge-transfer (CT) interactions in HFB·arene complexes. This leaves only electrostatic and van der Waals interactions to be considered. Brown and Swinton[19] suggested long ago that the attractive interactions between benzene and HFB molecules are predominantly electrostatic. The electrostatic forces between two molecules are dominated by the first non-vanishing electric moments, which for both benzene and HFB are the quadrupole moments, of similar (and rather large) magnitude and opposite sign.[20] Calculations of the quadrupole–quadrupole interactions between benzene and HFB molecules, separated by distances corresponding to a normal van der Waals contact, showed that the potential minimum corresponds to a parallel face-to-face orientation as observed in the solid state.[21] This minimum was also much deeper than those found for both pure benzene and pure HFB (which corresponded in both cases to a perpendicular arrangement of the molecules). Thus, quadrupole–quadrupole interactions were postulated as the cause of the higher stability of the complex in the solid state.[3b] Obviously, this reasoning can be extended to other arene-perfluoroarene complexes. An excellent review[4b] of aromatic interactions, covering the period 1950–2000, addresses the various forces governing these interactions. An even more recent quantitative study,[4d] combining NMR spectroscopy and extended electron density (XED) force-field calculations, gave results generally consistent with

† Presented at the 16th International Symposium on Fluorine Chemistry, University of Durham, Durham, UK, 16–21 July 2000, Abstract No. 309. For Part 7 see ref. 1.

‡ Electronic supplementary information (ESI) available: results of molecular thermal motion analysis and corrected bond distances, and intermolecular H···F contacts. See http://www.rsc.org/suppdata/nj/b2/b207102a/

 DOI: 10.1039/b207102a

the electrostatic model. However, the relative importance of electrostatic interactions has been questioned by some recent theoretical studies. Thus Lorenzo *et al.*[4a] calculated the intermolecular interaction energies in HFB·C_6D_6, $(HFB)_2$, $(C_6H_6)_2$ and $(OFN)_2$ dimers using Lennard–Jones potentials and the electrostatic energy in atom–atom approximation with atom partial charges estimated from various considerations including, for example, Mulliken, Hirshfeld and EPS charges derived from DFT calculations. They concluded that the electrostatic contribution is less that 15%, yet this result is strongly dependent on the choice of the atom partial charges. Lozman *et al.*[4c] performed similar calculations for these and other dimers using the XED model instead of atom centred charges, and suggested the van der Waals contribution predominates, although to a smaller degree.

In order to clarify this question, we undertook a systematic X-ray crystallographic and theoretical study of HFB·arene complexes. The earlier structural studies were confined to complexes of HFB with benzene and its methyl- and/or dimethylamino-substituted derivatives,[11–14,22] and with a few miscellaneous aromatics, such as hexamelamine,[8] (η^6-$C_6H_6)_2$-Cr,[23] (η^5-C_5Me_5)Co(acac)[24] or bis(*o*-diethynylbenzene).[25] In the latter complex, mixed stacks also exist, but the HFB molecule is stacked (exceptionally) against the central diyne bridges of the dimer, rather than one of its aromatic rings. To these, one can add some borane derivatives with *intra*molecular face-to-face stacking of phenyl and pentafluorophenyl substituents.[26]

Very little was known about the complexes of HFB with fused-ring polyaromatic molecules, although HFB·2-methylnapthalene was prepared early on by Patrick and Prosser[9] and found sufficiently stable (mp 56 °C) to be crystallised from ether, unlike HFB·benzene. The phase diagrams of binary mixtures of HFB with naphthalene[27] or 2-methylnaphthalene[28] show congruent melting points at equimolar composition. Boeyens and Herbstein[29] determined the unit cells of the HFB·anthracene, HFB·pyrene and HFB·perylene single-crystals and suggested that the structures may contain mixed stacks. In the present paper, we report the crystal structures of HFB·naphthalene (**1**), HFB·anthracene (**2**), HFB·phenanphenanthrene (**3**), HFB·pyrene (**4**) and HFB·triphenylene (**5**), which are discussed along with the previously reported[1] structure of HFB·acenaphthene, and *ab initio* DFT calculations on the crystal lattices of **1**, **2**, **4** and **5**. After this work had been completed, the crystal structures of **2** (at 245 K)[30] and **5** (at 85 K),[31] deposited by Day *et al.* in the Cambridge Structural Database, entered the public domain.

Experimental

The polyaromatic hydrocarbons (Aldrich) and hexafluorobenzene (Fluorochem) were tested for purity by GC-MS and used without further purification. GC-MS was carried out using a Hewlett-Packard HP-5890 Series II Gas Chromatograph equipped with a HP-5971A Mass Selective Detector. A 12 m fused silica (5% cross-linked phenylmethylsilicone) capillary column was used, with UHP grade helium as the carrier gas.

Single crystals of **1**–**5** were obtained by slow evaporation (over several weeks) of a solution containing 0.1 mmol of the corresponding arene in 1 ml of HFB. (*Caution:* many polyaromatics are carcinogenic and should be handled accordingly.) Crystals of **1**, **4**, and **5** were obtained as blocky needles, and those of **2** as irregular blocks and of **3** as thick plates. Crystals of **5** grew as non-merohedral twins, related by a 180° rotation around the c^* axis. Their diffraction patterns were deconvoluted and the twinning corrections made, using the GEMINI program.[32] However, the precision of the results is rather low due to a large number of partially overlapping reflections.

X-ray diffraction experiments (Table 1) for **1**, **3**, **4** and **5** were carried out on a SMART 3-circle diffractometer with a 1 K CCD area detector, using graphite-monochromated Mo-K_α radiation. Each data collection covered more than a hemisphere of reciprocal space by a combination of 4 sets of ω scans, each set at different φ and/or 2θ angles. Reflection intensities were integrated using SAINT software[33] and for **4** were corrected for absorption (mainly by the glass fibre) by a semi-empirical method based on Laue equivalents.[34] For **2**, the experiment was carried out on a Rigaku AFC6S 4-circle diffractometer, using graphite-monochromated Cu-K_α radiation. The data were processed using TEXSAN software.[35] An empirical (on ψ-scans) absorption correction was insignificant, $T_{min}/T_{max} = 0.89$. The crystals were cooled using

Table 1 Crystal data and structure refinement parameters

Complex	**1**	**2**	**3**	**4**	**5**
CCDC no.	175695	175696	175697	175698	175699
Formula	$C_6F_6{\cdot}C_{10}H_8$	$C_6F_6{\cdot}C_{14}H_{10}$	$C_6F_6{\cdot}C_{14}H_{10}$	$C_6F_6{\cdot}C_{16}H_{10}$	$C_6F_6{\cdot}C_{18}H_{12}$
M	314.22	364.28	364.28	388.30	414.34
T/K	180	150	120	200	120
Crystal system	Monoclinic	Monoclinic	Triclinic	Monoclinic	Monoclinic
Space group	$C2/c$ (#15)	$C2/c$ (#15)	$P\bar{1}$ (#2)	$P2_1/c$ (#14)	$P2_1/c$ (#14)
a/Å	11.806(1)	16.122(3)	6.929(2)	6.946(2)	13.935(2)
b/Å	13.508(1)	12.086(2)	7.308(1)	13.331(3)	7.211(2)
c/Å	8.426(2)	8.955(3)	15.991(3)	9.301(2)	17.370(8)
α/°	90	90	91.51(1)	90	90
β/°	97.15(1)	118.39(3)	102.16(1)	106.67(3)	92.55(1)
γ/°	90	90	100.16(1)	90	90
V/Å^3	1333.3(4)	1535.0(5)	777.5(3)	825.2(3)	1743.7(10)
Z	4	4	2	2	4
ρ_{calc}/g cm^{-3}	1.565	1.576	1.556	1.563	1.578
λ/Å	0.71073	1.54178	0.71073	0.71073	0.71073
μ/mm^{-1}	0.15	12.49	0.14	0.14	0.14
Reflections, total	4725	1608	9769	5231	10 590
Refls., unique	1530	1279	4080	1882	3075
R_{int}	0.050	0.045	0.034	0.033	0.144
Refls. with $I > 2\sigma(I)$	1083	1133	3056	1287	1722
R [$I > 2\sigma(I)$]	0.050	0.050	0.043	0.043	0.102
wR (F^2), all data	0.121	0.155	0.132	0.122	0.285

an Oxford Cryosystems open-flow N_2 gas cryostat;[36] the temperature was calibrated on the phase transition of K_2HPO_4 at 122.5 K,[37] the error not exceeding ±2 K. To avoid decomposition, the crystals were quickly transferred from HFB solutions directly into the jet of cold N_2.

All structures were solved by direct methods and refined by full-matrix least squares on F^2 of all data, using SHELXTL software.[38] All C and F atoms were refined in anisotropic approximation (isotropic for the minor position of the disordered phenanthrene molecule in **3**), H atoms in **1**, **2** and **4** were refined in isotropic approximation, and in **3** and **5** they were treated as 'riding'. Thermal motion analysis and bond length correction were made using PLATON-99 programs.[39] See electronic supplementary information (ESI)‡ for results of molecular thermal motion analysis and corrected bond distances, and intermolecular H···F contacts. CCDC reference numbers are given in Table 1. See http://www.rsc.org/suppdata/nj/b2/b207102a/ for crystallographic files in CIF or other electronic format.

Ab initio pseudopotential calculations within the DFT formalism were performed using the CASTEP code.[40] For a given configuration of the unit cell, expansion of the valence electronic wavefunction in a basis set of plane waves up to an energy cut-off of 400 eV, converged the total energy of the system to less than 1 meV cell^{-1}. Core electrons were described using the pseudopotential approach. The Vanderbilt[41] form for non-local ultrasoft pseudo-potentials was used. The Brillouin zone integrations were performed using a *k*-point set which converged the total energy of the system to less than 1 meV cell^{-1}. . For exchange and correlation interactions, the generalised gradient approximation (GGA)[42] was used, which is generally more accurate at describing molecular systems than the conventional local density approximation.[43] The total energy of the system was calculated by the preconditioned conjugate gradients method.[40]

Results and discussion

Colourless single crystals of HFB complexes, unlike those of the corresponding OFN complexes, are not air-stable. They can be preserved for a long time in the mother liquor or in the presence of HFB vapour, but otherwise decompose within seconds, leaving blocks of polycrystalline arene powder which retain the form of the original single-crystal. Insulating crystals with polyfluorinated oil did not prevent the loss of HFB; smaller single-crystals of arenes could be observed growing quickly out of a disintegrating crystal of the complex. Therefore, all of our experiments were performed at low temperatures. Only the HFB·naphthalene complex **1** gave a congruent mp of 94–95 °C. The others gave mps identical to those of the polyaromatic components, indicating loss of HFB.

Like all previously studied arene-perfluoroarene complexes, structures **1**–**5** display the mixed-stack packing motif. Molecular overlap is shown in Figs. 1 and 2, and assembly of stacks in a crystal, in Figs. 3 and 4. Complexes **1** and **2** both crystallise in space group $C2/c$, the HFB molecule lies on a crystallographic twofold axis [passing through C(1), C(4), F(1) and F(4)], while the naphthalene (in **1**) or anthracene (in **2**) molecule has a crystallographic inversion centre; the mixed stack is parallel to the [1 0 1] direction. In the triclinic structure of **3**, both the HFB and the phenanthrene molecules occupy general positions. The phenanthrene molecule is disordered between two co-planar and partially overlapping orientations, with occupancies of 87.3(2) and 12.7(2)%. Similar disorder was observed in OFN·phenanthrene,[2] and in the high-temperature phase of pure phenanthrene.[44] The stack in **3** is parallel to the *x* axis of the crystal. Complexes **4** and **5** both crystallise in the space group $P2_1/c$, but in **4** the HFB and the arene molecules lie at crystallographic inversion centres, while in **5** they have no crystallographic symmetry. The stack direction is parallel to the crystal *x* axis in **4**, and to the *y* axis in **5**.

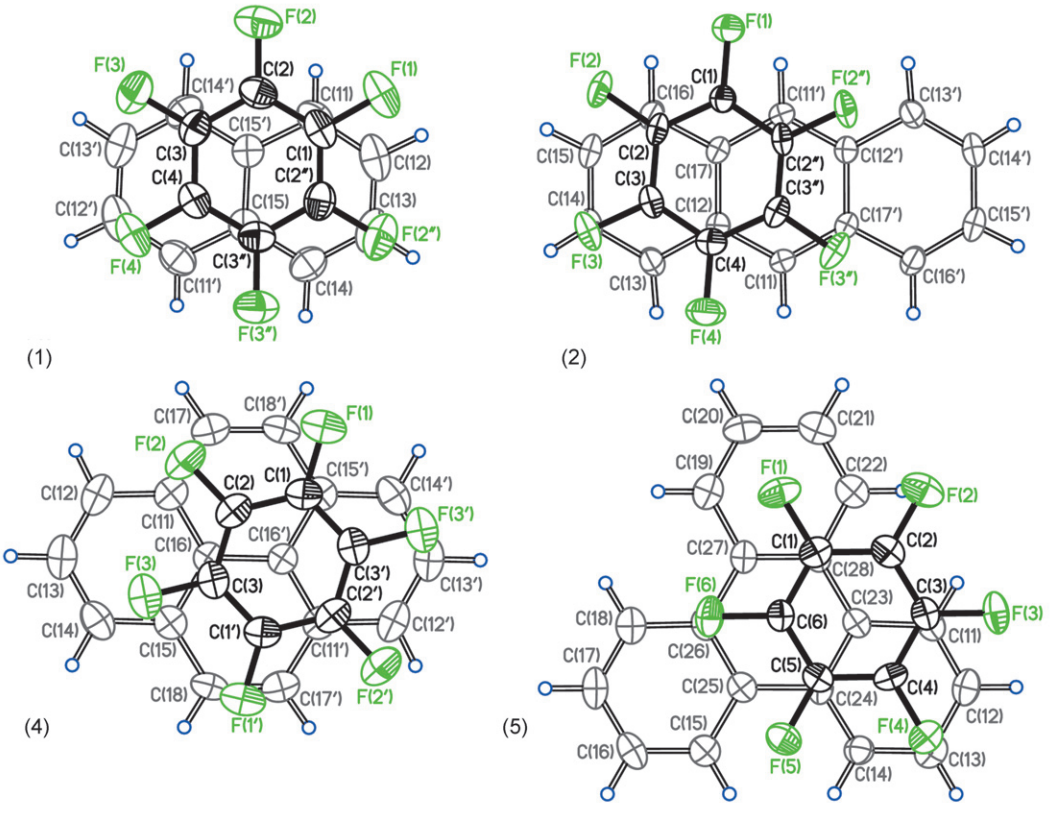

Fig. 1 Molecular structures of **1**, **2**, **4** and **5**. Atoms generated by inversion centres are primed, and those generated by twofold axes are double-primed. Thermal ellipsoids are drawn at the 50% probability level.

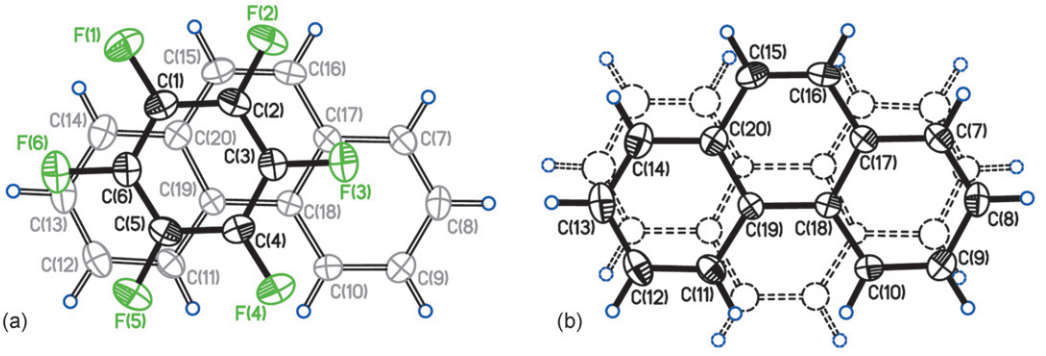

Fig. 2 Molecular structure of **3**. HFB showing the major phenanthrene position (a), and disorder of the phenanthrene molecule (b). Atoms in the minor positions are primed.

Due to easy rotation of the stacked molecules within their planes,[20] arene complexes with HFB (but not with more anisotropically shaped OFN) are prone to polymorphism. Indeed, we found that complex **1** undergoes a phase transition on cooling to *ca.* 175 K, whereupon the samples turned polycrystalline; only the high-temperature phase was studied (at 180 K). The *C*-centred monoclinic unit cell of **2**, measured at room temperature (on a single crystal sealed in a capillary),[29] is essentially the same as at 245 K[30] (see Table 2). The cell we found at 150 K is related to the former by a rational transformation $\mathbf{a} = -\mathbf{a}' - 2\mathbf{c}'$, $\mathbf{b} = \mathbf{b}'$, $\mathbf{c} = \mathbf{a}'$ (see Table 2 and Fig. 3; primed vectors refer to the high-temperature phase). In fact, the structures determined at 245 K[30] and 150 K are very similar (see Fig. 3), the main difference being a small (5°) rotation of the anthracene molecule. This obviously suggests that **2** undergoes a second-order phase transition on cooling. The uneven disorder of the phenanthrene molecule in **3** may also be the result of a phase transition, incomplete due to rapid cooling, as has been observed in pure phenanthrene.[44] The primitive unit cell of **4** did not change substantially between 200 K (the temperature of the structure determination) and 250 K (above which the crystals were not air-stable). However, at room temperature,[29] **4** has an *A*-centred cell of similar dimensions (apart from some shear deformation), again suggesting a phase transition with an increase of symmetry. On the other hand, the structures of **5** determined at 85 K[31] and 120 K (this work) are essentially the same.

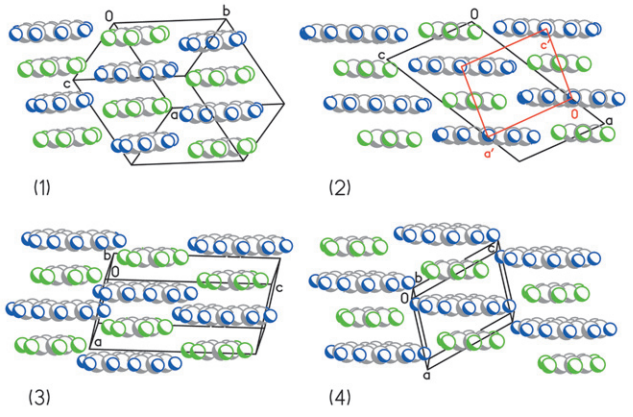

Fig. 3 Crystal packing of **1**–**4** (parallel projections). Note varying orientations of the naphthalene molecules in **1**. High-temperature unit cell of **2** is shown in red. Disorder of the phenanthrene molecules in **3** is omitted.

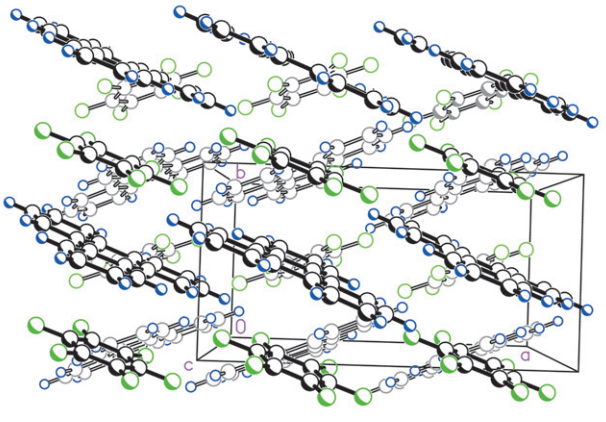

Fig. 4 Crystal packing of **5**, showing two adjacent layers.

Bond distances in **1**–**5** (see ESI‡) do not differ significantly from those in pure HFB[15] and pure arenes.[44,45] Some geometrical parameters describing the packing are compared in Table 3. In all complexes the interplanar angle (φ) between the adjacent molecules in the stack, is small. The average interplanar separation (d), as in the OFN complexes, is close to the van der Waals 'thickness' of an aromatic molecule (*ca.* 3.4 Å), *i.e.* consistent with a close packing without specific interactions. The stacks are not strictly columnar; the adjacent molecules are slipped parallel to each other's planes. The distortion, which can be described by the slip angle (θ) between the direction of the stack and the perpendiculars to the molecular planes, varies substantially between complexes. Interestingly, it tends to increase with the size of the arene molecule, while the opposite tendency was observed in the series of OFN·arene complexes.[2]

As we observed earlier, similar stacks can assemble differently in two or three dimensions. Let us assume, for simplicity, that all molecules within a stack are parallel ($\varphi = 0$). Columnar stacks ($\theta = 0$) can assemble into a layer only in such a way that all molecules within a layer are also parallel (Fig. 5*A*). Stacks with a slip can form two types of layers, with molecules of adjacent stacks being parallel (laminar motif, Fig. 5*B*) or inclined to one another (herringbone motif, Fig. 5*C*). Motifs *A* and *B* can also be characterised by a parallel shift (s) between adjacent stacks, assuming $s = 0$ if the arene molecule lies exactly in the plane of the perfluoroarene one. Obviously, for motif *C* this parameter is not meaningful. Layers of *A* or *B* type can be assembled in two ways: the next layer can be a parallel (*D*) or rotated (*E*) repetition of the previous one. These, of course, are idealised types; various intermediate motifs can also exist. Overall, the packing can be described by the 'spread' of molecular orientations, *i.e.* the maximum angle (ω) between the planes of any two molecules within the structure. This parameter can be relevant for useful bulk properties of the solids. Thus, parallelism of all molecular planes ($\omega = 0$) is one of the structural conditions for good thin-layer charge mobility.[46] It can also be assumed that

Table 2 Experimental and calculated unit cells of complexes **1**, **2**, **4** and **5**, calculated total cohesive energy per formula unit (E_t) and its Coulombic component (E_c)

	T/K	a/Å	b/Å	c/Å	β/°	Space group	E_t/eV	E_c/eV	Ref.
1	180	11.806	13.508	8.426	97.15	$C2/c$			This work
1	Calc.	11.821	13.533	8.451	97.94	$C2/c$	0.307	0.287	This work
2	295	9.03	12.2	7.26	95	$C2/m$			29
2	245	8.998	12.164	7.237	95.31	$C2/m$			30
2[a]	245	16.320	12.164	8.998	117.99				30
2	150	16.122	12.086	8.955	118.39	$C2/c$			This work
2	Calc.	16.136	12.128	8.984	117.19	$C2/c$	0.333	0.304	This work
4	295	6.98	13.5	9.88	113	$A2/m$[b]			29
4	200	6.946	13.331	9.301	106.67	$P2_1/c$			This work
4	Calc.	6.970	13.366	9.313	105.99	$P2_1/c$	0.358	0.327	This work
5	120	13.935	7.211	17.370	92.55	$P2_1/c$			This work
5	85	13.584	7.179	17.256	92.98	$P2_1/c$			31
5	Calc.	13.959	7.241	17.393	92.66	$P2_1/c$	0.371	0.341	This work

[a] After the transformation $\mathbf{a} = -\mathbf{a}' - 2\mathbf{c}'$, $\mathbf{b} = \mathbf{b}'$, $\mathbf{c} = \mathbf{a}'$. [b] Or $A2$, or Am, from systematic absences.

systems with $\omega \approx 0$ in the solid state are more likely to form laminar liquid crystals.

In structure **1**, the stacks show little slip and the layer configuration closely approaches type *A*, while in complexes **2**–**5**, with larger slips, it is of type *B*. In each structure, HFB molecules of one stack lie closer to the arene (rather than HFB) molecules of adjacent stacks, but not exactly opposite to them. Such a configuration is probably due to a compromise between electrostatic attraction between H and F atoms (tendency toward $s = 0$) and the gain of packing density when a molecule fits a gap in the adjacent stack (tendency toward $s = d/2$). This results in a number of inter-stack contacts between oppositely charged H and F atoms (see ESI‡), whose electrostatic attraction may play some role in stabilising the solid-state structures of the complexes.[47] The roughly inverse relationship between θ and s (Table 3) can be understood from simple geometrical considerations, as the simultaneous large slip and shift would lead to excessively short intermolecular contacts.

In structures **1**, **2** and **4**, the monoclinic (twofold) axis is perpendicular to the stack direction and (rigorously or approximately) parallel to the molecular planes, hence the molecules in adjacent layers are parallel (Fig. 5, *D*). The same mode of packing directly follows from the triclinic symmetry of structure **3**. Thus, complexes **1**–**4** are similar to OFN·arene complexes (except OFN·naphthalene) which show a motif *A* or *B* within a layer and *C* between the layers. On the other hand, in **5**, the monoclinic axis is parallel to the stack direction, hence the (equivalent) molecules of adjacent layers form an interplanar angle equal to twice the slip angle. Structure **5** thus belongs to class *E*, like OFN·naphthalene and its analogues (*vide supra*), although the angular spread, ω, in **5** is larger (46.9°) than in these complexes (34.3–34.7°).

The *ab initio* calculations for **1**, **2**, **4** and **5** (excluding the disordered **3**) were performed by time-independent DFT method in the generalised gradient approximation (GGA). The method uses periodic boundary conditions to simulate the infinite crystal. This includes all interactions of the infinite atom system, which is implemented by the use of Bloch's theorem for a periodic system. The forces on the atoms and stresses on the unit cell are calculated by *ab initio* methods using the Hellmann–Feynman theorem. From this we were able to calculate the fully relaxed crystal structure, *i.e.* to refine the unit cell parameters and the atomic positions, taking the experimental structure as the starting point. The resulting parameters (Table 2 and ESI‡) coincide with the experimental ones within 1%. Usually the DFT GGA method describes van der Waals (dispersion) interactions poorly, resulting in gross overestimation of the equilibrium distances of purely van der Waals interactions, *e.g.* interatomic distances in (condensed-phase) inert gases or interplanar separations in graphite.[48] No such overestimation occurs in the present case; this can be taken as an indirect evidence that the cohesion is predominantly of electrostatic, rather than van der Waals, character.

Having integrated the calculated electron charge density over each molecule in the unit cell, we found that molecules of HFB as well as arenes in each of the complexes are neutral within the accuracy of the calculation ($< 0.01\ e^-$), *i.e.* charge transfer plays no role in the cohesion. Thereupon we calculated the electrostatic energy directly, using the entire charge density distribution in the molecules, as determined in the DFT study (rather than atom-centred charges or multipole representations). Thus, in an important contrast to previous approaches, from the *ab initio* calculations used in the present work, there

Table 3 Stacking geometry in **1**–**5**[a]

Complex	**1**	**2**	**3**[b]	**4**	**5**
φ/°	2.5	1.5	1.0	0.6	1.5
θ/°	4.4	20.4	14.2	12.4	23.1
ω/°	3.6	2.5	1.0	1.1	46.9
d/Å	3.40	3.34	3.36	3.39	3.31
s/Å	1.5	0.6	1.0	1.1	0.9

[a] φ – angle between adjacent arene and perfluoroarene molecular planes within a column; ω – maximum angle between planes of any two molecules within the structure; for definitions of θ, d and s, see Fig. 4. For non-parallel molecules d is defined as the average of the distances between the centroid of one molecule and the mean plane of another. [b] For the major position of the phenanthrene molecule.

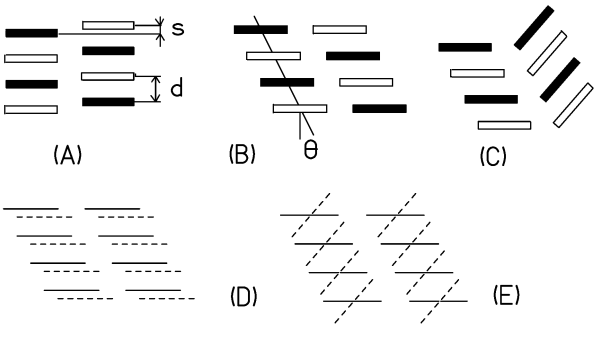

Fig. 5 Packing motifs of arene-perfluoroarene complexes. For *A*, *B* and *C*, arene molecules are shown in white, and perfluoroarene in black; for *D* and *E*, molecules of the front layer are solid, and those of the rear layer are dashed.

was no need to artificially assign partial charges to atoms, as we have (i) the electronic charge density of each molecule in the material, stored on a grid with *ca.* 12 grid points/Å (the size of the subdivision is defined by the basis cut-off); and (ii) the position of the positive ionic core. We therefore used this information to calculate the electrostatic energy between molecules using the same (Coulomb's law) classical electrostatic method as one would have used for partial atom charges. The resulting values are listed in Table 2, alongside the total cohesion energies calculated by the DFT method. It appears that electrostatic attraction contributes more than 90% of the total cohesion. We also obtained the electrostatic potentials for the four complexes. Fig. 6 (a,b) illustrates the potentials on the HFB and naphthalene molecules respectively in complex **1**. The deepest minima of the potential are located on the two central carbon atoms, *i.e.* C(15) and C(15′), of the naphthalene molecule and on the fluorine atoms of the HFB. Comparison of Fig. 6 (a,b) with Fig. 1 shows that molecules in the stack overlap in such a way as to maximise the distances between the minima of the electrostatic potential, *i.e.* the centres of the highest negative charge. The corresponding maps for anthracene, pyrene and triphenylene in structures **2**, **4** and **5** are given in Fig. 6 (c,d,e); the electrostatic potential distribution for HFB in all four complexes differs insignificantly. Clearly, the position of the HFB relative to the arene (within a stack) is governed by electrostatic forces (see also ref. 25).

Thus, we found the ratio of the van der Waals and Coulombic contributions, to be the reverse of that found in some recent quantitative computations,[4a,c] although essentially in agreement with the earlier qualitative conclusions.[3b,19] In our view, the techniques employed by Lorenzo *et al.*[4a] and Lozman *et al.*[4c] have a number of shortcomings, which makes their results less reliable. Firstly, atom-centred charges (ACC) constitute a very crude model for Coulombic energy calculations. Furthermore, in polar-covalent *and* aromatic molecules the partition of continuous electron density into atomic charges is always to a considerable degree arbitrary. The XED model is a substantial improvement upon the ACC, and it is noteworthy that the former gives a much higher proportion of the electrostatic contribution: for HFB·benzene, 27% (XED) against 22% (ACC), for perfluorotriphenylene·triphenylene, 29% (XED) against 16% (ACC).[4c] Still, the XED representation used by Lozman *et al.* is a much rougher approximation than the one used in this work. It is noteworthy that the multipole approximation has its own limitations: dependence on the order of the multipoles selected and the fact that only the first non-vanishing term is origin-independent. There are also problems with this description when the intermolecular distances are comparable to molecular size. Finally, all previous calculations referred to isolated pairs or small clusters of molecules in the gas phase (rather than continuous solid-state packing, as in our study), thereby neglecting all long-range interactions and some important short-range ones, particularly the inter-stack H···F contacts, which can contribute to the electrostatic attraction (*vide supra*). It has already been noted that apparently simple arene-perfluoroarene complexes, even HFB·benbenzene, require very high levels of theory to predict the experimental observations,[3c] and it has been pointed out that low-level *ab initio* calculations can be even qualitatively wrong.[4c]

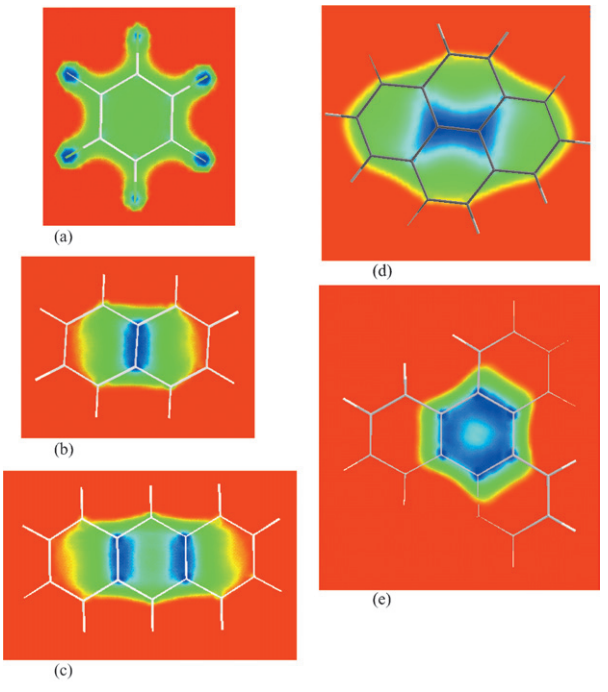

Fig. 6 Calculated electrostatic potentials of the molecules of HFB (a) and naphthalene (b) in the crystal of **1**, anthracene in **2** (c), pyrene in **4** (d) and triphenylene in **5** (e), in cross-sections through the mean molecular planes.

Conclusions

We have shown that HFB can form distinct 1:1 complexes, broadly similar to the complexes formed by OFN, with a number of fused-ring aromatic molecules of varying size and shape. The solid-state structures of these complexes, as of all previously studied analogues, contain mixed stacks of alternating parallel arene and perfluoroarene molecules, quite different from the (usually herringbone) packing of the pure components. These stacks constitute an important synthon for crystal engineering. Another recurrent feature of arene-perfluoroarene complexes is a layer of stacks, in which all molecular planes are approximately parallel. However, the structures display different slip angles within a stack, as well as different 3-dimensional packing modes, which show no simple dependence upon the nature and relative size of the components. The *ab initio* calculations give strong reasons to believe that the packing mode is governed mainly by electrostatic interactions, which should be taken into account in any attempt to understand the supramolecular organisation of these complexes.

Acknowledgements

The EPSRC is gratefully acknowledged for a Senior Research Fellowship (JAKH) and a postgraduate studentship (JCC).

References

1 J. C. Collings, A. S. Batsanov, J. A. K. Howard and T. B. Marder, *Cryst. Eng.*, 2002, **5**, 37.
2 J. C. Collings, K. P. Roscoe, R. Ll. Thomas, A. S. Batsanov, L. M. Stimson, J. A. K. Howard and T. B. Marder, *New J. Chem.*, 2001, **25**, 1410.
3 (*a*) T. Dahl, *Acta Crystallogr., Sect. B*, 1990, **46**, 283; (*b*) J. H. Williams, *Acc. Chem. Res.*, 1993, **26**, 593; (*c*) A. P. West Jr., S. Mecozzi and D. A. Dougherty, *J. Phys. Org. Chem.*, 1997, **10**, 347.
4 (*a*) S. Lorenzo, G. R. Lewis and I. Dance, *New J. Chem.*, 2000, **24**, 295; (*b*) C. A. Hunter, K. R. Lawson, J. Perkins and C. J. Urch, *J. Chem. Soc., Perkin Trans. 2*, 2001, 651; (*c*) O. R. Lozman, R. J. Bushby and J. G. Vinter, *J. Chem. Soc., Perkin Trans. 2*, 2001, 1446; (*d*) H. Adams, J.-L. J. Blanco, G. Chessari, C. A. Hunter, C. M. R. Low, J. M. Sanderson and J. G. Vinter, *Chem. Eur. J.*, 2001, **7**, 3494.
5 (*a*) G. W. Coates, A. R. Dunn, L. M. Henling, D. A. Dougherty and R. H. Grubbs, *Angew. Chem., Int. Ed. Engl.*, 1997, **36**, 248; (*b*) G. W. Coates, A. R. Dunn, L. M. Henling, J. W. Ziller, E. B. Lobkovsky and R. H. Grubbs, *J. Am. Chem. Soc.*, 1998, **120**, 3641; (*c*) A. F. M. Kilbinger and R. H. Grubbs, *Angew. Chem., Int. Ed.*, 2002, **41**, 1563.

6 M. L. Renak, G. P. Bartholomeu, S. Wang, P. J. Ricatto, R. J. Lachicotte and G. C. Bazan, *J. Am. Chem. Soc.*, 1999, **121**, 7787; W. J. Feast, P. W. Lovenlich, H. Puschmann and C. Taliani, *Chem. Commun.*, 2001, 505.
7 C. Dai, P. Nguyen, T. B. Marder, A. J. Scott, W. Clegg and C. Viney, *Chem. Commun.*, 1999, 2493; M. Weck, A. R. Dunn, K. Matsumoto, G. W. Coates, E. B. Lobkovsky and R. H. Grubbs, *Angew. Chem., Int. Ed.*, 1999, **38**, 2741.
8 M. J. Aroney, T. W. Hambley, E. Patsalides, R. K. Pierens, H.-K. Chan and I. Gonda, *J. Chem. Soc., Perkin Trans. 2*, 1987, 1747.
9 C. R. Patrick and G. S. Prosser, *Nature*, 1960, **187**, 1021.
10 D. F. R. Gilson and C. A. McDowell, *Can. J. Chem.*, 1966, **44**, 945; J. A. Ripmeester, D. A. Wright, C. A. Fyfe and R. K. Boyd, *J. Chem. Soc., Faraday Trans. 2*, 1978, **74**, 1164; J. A. Williams, *Mol. Phys.*, 1991, **73**, 99–113; J. S. W. Overell and G. S. Pawley, *Acta Crystallogr., Sect. B*, 1982, **38**, 1966.
11 J. H. Williams, J. K. Cockcroft and A. N. Fitch, *Angew. Chem., Int. Ed. Engl.*, 1992, **31**, 1655.
12 T. Dahl, *Acta Chem. Scand.*, 1971, **25**, 1031; T. Dahl, *Acta Chem. Scand.*, 1972, **26**, 1569; T. Dahl, *Acta Chem. Scand.*, 1973, **27**, 995; T. Dahl, *Acta Chem. Scand.*, 1975, **A29**, 170; T. Dahl, *Acta Chem. Scand.*, 1975, **A29**, 699.
13 N. Boden, P. P. Davis, C. H. Stam and G. A. Wesselink, *Mol. Phys.*, 1973, **25**, 81; M. D. Bertolucci and R. E. Marsh, *J. Appl. Crystallogr.*, 1974, **7**, 87.
14 G. R. Desiraju and A. Gavezzotti, *Acta Crystallogr., Sect. B*, 1989, **45**, 473.
15 J. Potenza and D. Mastropaolo, *Acta Crystallogr., Sect. B*, 1975, **31**, 2527.
16 A. S. Batsanov, J. C. Collings, J. A. K. Howard and T. B. Marder, *Acta Crystallogr., Sect. E*, 2001, **57**, 950.
17 D. S. Yufit, J. C. Collings, J. A. K. Howard and T. B. Marder, unpublished results.
18 M. E. Baur, D. A. Horsma, C. M. Knobler and P. Perez, *J. Phys. Chem.*, 1969, **73**, 641; M. E. Baur, C. M. Knobler, D. A. Horsma and P. Perez, *J. Phys. Chem.*, 1970, **74**, 4594.
19 N. M. D. Brown and F. L. Swinton, *J. Chem. Soc., Chem. Commun.*, 1974, 770.
20 (*a*) M. R. Battaglia, A. D. Buckingham and J. H. Williams, *Chem. Phys. Lett.*, 1981, **78**, 421; (*b*) J. Vrbancich and G. L. D. Ritchie, *J. Chem. Soc., Faraday Trans. 2*, 1980, **76**, 648.
21 J. Hernandez-Trujillo, M. Costas and A. Vela, *J. Chem. Soc. Faraday Trans.*, 1993, **89**, 2441.
22 T. G. Beaumont and K. M. C. Davis, *J. Chem. Soc. B*, 1967, 1131.
23 C. J. Aspley, C. Boxwell, M. L. Buil, C. L. Higgit, C. Long and R. N. Perutz, *Chem. Commun.*, 1999, 1027.
24 J. J. Schneider, R. Goddard and C. Kruger, *Z. Naturforsch., B*, 1995, **50**, 448.
25 U. H. F. Bunz and V. Enkelmann, *Chem. Eur. J.*, 1999, **5**, 263.
26 D. J. Parks, W. E. Piers, M. Parvez, R. Atencio and M. J. Zaworotko, *Organometallics*, 1998, **17**, 1369; J. M. Blackwell, W. E. Piers, M. Parvez and R. McDonald, *Organometallics*, 2002, **21**, 1400.
27 E. McLaughlin and C. E. Messer, *J. Chem. Soc. A*, 1966, 1106.
28 G. Griffith, P. R. Jackson, E. Kenyon-Blair and K. W. Morcom, *J. Chem. Thermodyn.*, 1983, **15**, 1001.
29 J. C. A. Boeyens and F. H. Herbstein, *J. Phys. Chem.*, 1965, **69**, 2153.
30 M. W. Day, A. J. Matzger and R. H. Grubbs, Private communication to CCDC, 2002, ref.code ZZZGMW01.
31 M. W. Day, A. J. Matzger and R. H. Grubbs, Private communication to CCDC, 2002, ref.code MIVRAK.
32 GEMINI, version 1.0, Bruker AXS, Madison, WI, USA, 1999–2000.
33 SAINT, version 6.01, Bruker AXS, Madison, WI, USA, 1999.
34 G. M. Sheldrick, SADABS, University of Göttingen, Germany, 1998.
35 TEXSAN, version 5.1, MSC, The Woodlands, TX, USA, 1989.
36 J. Cosier and A. M. Glazer, *J. Appl. Crystallogr.*, 1986, **19**, 105.
37 R. J. Nelmes, G. M. Meyer and J. E. Tiballis, *J. Phys. C*, 1982, **15**, 59.
38 SHELXTL, version 5.10, Bruker AXS, Madison, WI, USA, 1997.
39 A. L. Speck, PLATON-99, Univ. of Utrecht, The Netherlands, 1980–1999.
40 CASTEP v.4.2, Academic version licensed under the UKCP-MSI Agreement, 1999; M. C. Payne, M. P. Teter, D. C. Allan, T. A. Arias and J. D. Joannopolous, *Rev. Mod. Phys.*, 1992, **64**, 1045; M. D. Segall, P. L. D. Lindan, M. J. Probert, C. J. Pickard, P. J. Hasnip, S. J. Clark and M. C. Payne, *J. Phys. Cond. Matt.*, 2002, **14**, 2717.
41 D. Vanderbilt, *Phys. Rev.*, 1990, **B41**, 7892.
42 J. P. Perdew, *Electronic Structure of Solids 1991*, ed. P. Ziesche and H. Eschrig, Academie Verlag, Berlin, 1991; J. P. Perdew, J. A. Chevary, S. H. Vosko, K. A. Jackson, M. R. Pederson, D. J. Singh and C. Fiolhais, *Phys. Rev. B*, 1992, **46**, 6671.
43 J. P. Perdew and A. Zunger, *Phys. Rev. B*, 1981, **23**, 5048.
44 V. Petricek, I. Cisarova, L. Hummel, J. Kroupa and B. Brezina, *Acta Crystallogr., Sect. B*, 1990, **46**, 830.
45 (*a*) C. P. Brock and J. D. Dunitz, *Acta Crystallogr., Sect. B*, 1982, **38**, 2218; (*b*) C. P. Brock and J. D. Dunitz, *Acta Crystallogr., Sect. B*, 1990, **46**, 795; (*c*) G. Ferraris, D. W. Jones and J. Yerkess, *Z. Kristallogr.*, 1973, **138**, 113; (*d*) Y. Kai, F. Hama, N. Yasuoka and N. Kasai, *Acta Crystallogr., Sect. B*, 1978, **34**, 1263.
46 G. Horowitz, *Adv. Mater.*, 1998, **10**, 365.
47 L. Shimoni and J. P. Glusker, *Struct. Chem.*, 1994, **5**, 383; V. R. Thalladi, H.-C. Weiss, D. Blaser, R. Boese, A. Nangia and G. R. Desiraju, *J. Am. Chem. Soc.*, 1998, **120**, 8702.
48 (*a*) P. Garcia-Gonzalez and R. W. Godby, *Phys. Rev. Lett*, 2002, **88**, 056 406; (*b*) N. Kurita and H. Sekino, *Chem. Phys. Lett.*, 2001, **348**, 139.